EUROPEAN ORGANIZATION FOR NUCLEAR RESEARCH

CERN-EP/87-183
30 September 1987

REMEASUREMENT OF THE MAGNETIC MOMENT OF THE ANTIPROTON*

A. Kreissl[1], A.D. Hancock[2], H. Koch, Th. Köhler, H. Poth, U. Raich[3], D. Rohmann[4] and A. Wolf
Kernforschungszentrum Karlsruhe, Institut für Kernphysik, and
Universität, Institut für Experimentelle Kernphysik, Karlsruhe,
Fed. Rep. Germany

L. Tauscher
Institute for Physics, University of Basle, Switzerland

A. Nilsson
Research Institute of Physics, Stockholm, Sweden

M. Suffert
Centre de Recherches Nucléaires, Strasbourg, France

M. Chardalas and S. Dedoussis
Department of Nuclear Physics, University of Thessaloniki, Greece

H. Daniel, T. von Egidy, F.J. Hartmann, W. Kanert, H. Plendl[5] and G. Schmidt
Physik Department, Technische Universität München,
Munich, Fed. Rep. Germany

J.J. Reidy
Physics Department, University of Mississippi, University, Mississipi, USA

(Submitted to Zeitschrift für Physik C)

---

* This publication forms part of the thesis of A. Kreissl

[1] Now at QUANTRONIX, Darmstadt, FRG

[2] Now at EG & G, Los Alamos, New Mexico, USA.

[3] Now at CERN, Geneva, Switzerland.

[4] Now at University of Bochum, Bochum, FRG.

[5] Permanent address: Physics Department, Florida State University, Tallahassee, Florida, USA.

ABSTRACT

A high-precision measurement of the fine-structure splitting in the circular 11 → 10 X-ray transition of $\bar{p}^{208}Pb$ was performed. The experimental value of 1199(5) eV is in agreement with QED calculations. From that value the magnetic moment of the antiproton was deduced to be $-2.8005(90)\ \mu_{nucl}$. With this result the uncertainty of the previous world average value was reduced by a factor of $\approx$ 2. A comparison with the corresponding quantity of the proton now yields: $(\mu_p - |\langle\mu_{\bar{p}}\rangle|)/\mu_p = (-2.4 \pm 2.9) \times 10^{-3}$.

1. INTRODUCTION

The method using exotic atoms is a proven means of determining elementary-particle properties and of studying hadron–nucleon interactions at rest. Owing to the spin $^1/_2$ of the antiproton the atomic levels are split into two components, with the spin parallel to the angular momentum in the more weakly bound state. From the size of this splitting, deduced from the energies of X-ray transitions populating the atomic level under consideration, the magnetic moment of the antiproton can be obtained. The fine-structure splitting usually amounts to roughly 1% of the total binding energy of the states. With the resolution of solid-state detectors one can resolve the X-ray multiplet only for heavy $\bar{p}$ atoms. Since antiprotons interact also through strong interaction with nucleons, deeply bound atomic states are perturbed; they are shifted in energy and broadened. Hence one has to choose a highly excited atomic state where the strong interaction does not play any role. In the measurement presented here the $11 \rightarrow 10$ transition $\bar{p}^{208}$Pb was selected.

The pure low-energy $\bar{p}$ beam delivered by the Low-Energy Antiproton Ring (LEAR) at CERN made a remeasurement of the magnetic moment of the antiproton attractive. It was possible to use a thin isotopically pure ^{208}Pb target so as to reduce background and systematic errors considerably. Preliminary results were already presented elsewhere [1, 2].

A precise measurement of the $\bar{p}$ magnetic moment always allows the validity of the CPT theorem to be tested by comparison with the corresponding quantity for the proton. However, one is also interested in the detection of binding effects since the antiproton is off-shell in the $\bar{p}$–nucleus system. This certainly affects the magnetic moment, as in the case of muonic atoms [3]. In $\bar{p}$ atoms, however, other effects should show up in addition, which reflect the hadronic nature of the antiproton [4].

2. THE ELECTROMAGNETIC $\bar{p}$ LEVELS AND X-RAY TRANSITIONS

The motion of a spin-$^1/_2$ particle in a Coulomb potential is described by the Dirac equation. Different from the electron the antiproton has a large anomalous magnetic moment. The total magnetic moment is

$$\mu_{\bar{p}} = -(1 + \varkappa)\mu_{\text{nucl}} \ . \tag{1}$$

The solution of the Dirac equation for a point nucleus given in Pauli approximation [5] is

$$\Delta E_{n\ell} = (1 + 2\varkappa)\,(mc^2/2)\,\{(Z\alpha)^4/[n^3\ell(\ell + 1)]\} \ , \tag{2}$$

where m is the reduced mass of the $\bar{p}$–nucleus system, and n and ℓ are the principal and orbital angular momentum quantum numbers, respectively.

On the other hand, the eigenvalue problem for the Dirac equation can be written as follows, including also higher QED corrections [6, 7]:

$$E|\psi\rangle = (T + V_{\text{Coul}} + V_{\varkappa} + V_{\text{vpl}} + V_{\text{pert}})|\psi\rangle \ . \tag{3}$$

Here T and V_{Coul} are the kinetic energy and the Coulomb potential, respectively. The term $V_{\varkappa}$ describes the contribution of the anomalous magnetic moment and V_{vpl} contains the vacuum polarization of the order of $\alpha Z\alpha$ and $\alpha Z\alpha^2$. Finally V_{pert} denotes correction terms that can be treated as perturbations, including, in general, vacuum polarization up to the order of $\alpha(Z\alpha)^7$, the finite-size effect, the electric and magnetic hyperfine structure, electron screening, recoil corrections, and nuclear polarizability. The author of Refs. [6, 7] has integrated the Dirac equation numerically and calculated the fine-structure splitting for various $\bar{p}$ atoms under the assumption that $\varkappa$ (= 1.7928456) is the same for the proton and the antiproton.

The fine-structure formula given by Bethe and Salpeter [Eq. (2)] was extended to include recoil contributions [8].

$$\Delta E_{n\ell} = [1 + 2\varkappa(m/m_{\bar{p}})]\,(mc^2/2)\,\{(Z\alpha)^4/[n^3\ell(\ell + 1)]\}\ . \tag{4}$$

This was then extended to include also vacuum polarization [9]. In a recent paper the fine structure in $\bar{p}$ atoms was calculated perturbatively to higher order in the vacuum polarization potential, and in relativity, including all orders of recoil corrections for light [10] and heavy [11] $\bar{p}$ atoms.

For the determination of the magnetic moment, only those atomic levels were considered where the strong interaction is negligible. The allowed transitions a, b, and c, between two levels, are shown in Fig. 1. By measuring the energy difference between the components of the triplet, $\varkappa$ can be determined directly. In the absence of disturbing effects, the intensity ratio of these transitions is given by the relation

$$I_a : I_b : I_c = j(2j + 3) : 1 : [j(2j + 1) - 1]\ , \tag{5}$$

which shows the dominance of the two components a and c with increasing total angular momentum j (choice of j in Fig. 1).

For the selection of a transition to be measured with high precision, it is important that the energy difference between these components be larger than the detector resolution. As is obvious from Eq. (4), this can be achieved by selecting a heavy nucleus. Moreover, there should be no hyperfine structure (vanishing nuclear spin) in order to have only three X-ray transition components. Also this X-ray region should be free from disturbing X-rays or nuclear γ-rays. The transitions $12 \rightarrow 11$ (222.2 keV) and $11 \rightarrow 10$ (292.5 keV) in $\bar{p}^{208}$Pb fulfilled these conditions and were selected as candidates.

3. THE APPARATUS

The experimental set-up consisted of a scintillator telescope, a wedge-shaped polyethylene degrader, and a target of circular shape. Five high-purity Ge semiconductor detectors (D1–D5) were placed around this target. An incoming antiproton was defined by the coincidence signal of the two scintillation counters. The degrader was used to slow down the antiprotons in order to let them stop in the 300 mg/cm^2 metallic target (diameter 3 cm). The $\bar{p}$ X-rays were detected in a range up to 675 keV. The characteristic data of the detectors are given in Table 1. The electronics and data-acquisition system are described elsewhere in detail [1, 12–14].

The data were taken during two LEAR running periods at $\bar{p}$ momenta of 200 MeV/c and 300 MeV/c. A total of 654 million antiprotons were stopped.

4. DATA ANALYSIS

The evaluation of the X-ray spectra was done as described elsewhere in more detail [12, 13]. We shall give in the following just a brief summary.

4.1 The calibration

The Ge detectors were first calibrated with standard radioactive sources of ^{75}Se, ^{133}Ba, and ^{241}Am, when the beam was off. This was taken as a zero-order calibration. For the final in-beam calibration those $\bar{p}^{208}$Pb X-ray transitions were taken which were not perturbed by the strong interaction. The calibration peaks were fitted with a single Gaussian line and a linear background. In all cases it was sufficient to use a linear polynomial for the energy calibration. The detector resolution as a function of energy was also determined from these fits.

4.2 Evaluation of the $\bar{p}^{208}$Pb 11 → 10 lines

Each observed X-ray transition n → n − 1 consists, in principle, of one circular transition (between levels with maximal angular momentum) and parallel transitions, all having components a, b, and c. Only parallel transitions with more than 1% of the total peak intensity were included in the fit. It turned out that only the circular transition $|n, \ell = n - 1\rangle \rightarrow |n' = n - 1, \ell' = n - 2\rangle$ and the first parallel transition $|n, \ell = n - 2\rangle \rightarrow |n' = n - 1, \ell' = n - 3\rangle$ of the $\bar{p}$ ^{208}Pb 11 → 10 transition had to be taken into account.

Since the intensity of component b is less than 3‰ of the total intensity of the 11 → 10 transition and its energy value is well outside the doublet, only components a and c were considered in the fit. For all fits the background was assumed to be linear. For the final determination of the $\bar{p}$ magnetic moment only the 11 → 10 transition in $\bar{p}^{208}$Pb was evaluated, since the 12 → 11 line could not be resolved by any of the detectors used. Figure 2 shows the two transitions for one of the detectors used.

Initially the fit was done with the energies of the two main components of the circular and first non-circular transitions set to the theoretical value [15, 16]. The Gauss widths were set equal for all four peaks and varied together in the fit. Finally the intensity ratios of the fine-structure components were set to the value given by Eq. (5). In this way the intensity of the first non-circular transition I^{1PT} could be determined directly from the measured line doublet, since the fit was very sensitive to the energy differences between the circular and the parallel transitions. Its contribution to the total intensity was found to be $I^{1PT}:I^{circ} = 3.8\% \pm 1.1\%$ (average of all detectors). This method has the advantage of being independent of cascade calculations and is thus model independent.

In a second step, the positions and the intensities of the first non-circular doublet were fixed and only the circular transitions were fitted, with their energy being varied independently. The intensity ratio $I_a^{circ}:I_c^{circ}$ so deduced corresponds to a statistical population in the $n = 10, \ell = 9$ level. As a check then the intensity of the first parallel transition was computed again with the energy and intensity values of the circular transition from the second approach as input. The variation of the intensity was found to be negligible with respect to the given error.

The total experimental error of the fine-structure-splitting measurement in the circular transitions contains, besides the statistical uncertainty, (i) the calibration error, (ii) the uncertainty of line-shape corrections, (iii) the uncertainty in the intensity of the parallel transition, and (iv) the error due to the variation of the widths of the fit region each one being of the order of 2 eV. These errors have been added in quadrature for each detector. In Table 2 the final fine-structure splitting determined for each detector is given. All values agree within the errors. Their weighted mean is also given in Table 2, together with the intensity ratio and the ratio of the first non-circular to the circular doublet.

5. RESULTS AND DISCUSSION

The fine-structure splitting of the $\bar{p}$ 11 → 10 transition in ^{208}Pb was measured to be $\Delta E = (1199 \pm 5)$ eV. This agrees well with the numerical QED calculation by Borie [6], who obtained $\Delta E = 1196$ eV, and with the perturbative evaluation by Bohnert et al. [11], who obtained $\Delta E = 1194.8$ eV. In both calculations $\varkappa$ was the same for protons and antiprotons. (Moreover, note that using Eq. (2) one arrives at a value of $\Delta E = 1171$ eV when using the $\varkappa$ value of 1.7928456.) On the other hand, by adjusting $\varkappa$ so that the numerical calculation of Ref. [6] reproduces the measured fine-structure splitting, one finds for $\varkappa$ the value 1.800 ± 0.009 while the adjustment to the analytical calculation of Ref. [11] leads to the value 1.801 ± 0.009. Consequently, for the magnetic moment of the antiproton, we have an average value of

$$\mu_{\bar{p}} = -2.8005(90)\, \mu_{nucl} \ .$$

This compares well with previous measurements [17, 18]; however the uncertainty is reduced by a factor of ≈ 2. The magnetic moment of the proton [19] has the value

$$\mu_p = 2.7928456(11)\,\mu_{nucl} \ .$$

Hence we confirm that the absolute value of the magnetic moments of the proton and the antiproton are in agreement within 2.9×10^{-3}:

$$(\mu_p - |\langle\mu_{\bar{p}}\rangle|)/\mu_p = (-2.4 \pm 2.9) \times 10^{-3} \ .$$

This result is equivalent to an equally precise CPT test for this baryonic property. The agreement with the theoretical calculations [6, 11], which do not include binding effects, leads us to the conclusion that those effects as observed for the bound muon [20, 21] and as conjectured for bound nucleons [4] do not alter the fine-structure splitting in heavy $\bar{p}$ atoms nor do $\bar{p}$ binding effects change the magnetic moment of the antiproton at this level of precision.

The uncertainty is still mainly limited by statistics. We hope to reduce it in the future with results from further measurements of the fine-structure splitting in $\bar{p}$ ^{174}Yb, ^{232}Th, and ^{238}U.

Acknowledgements

We would like to thank D. Simon, D. Dumollard and the LEAR staff for their collaboration during the data taking of this experiment. The numerical calculations of the antiprotonic energy eigenvalues were done by E. Borie and B. Jödicke. For technical assistance we are grateful to H. Hagn, J. Hauth and M. Meyer. The work was supported by the Bundesministerium für Forschung und Technologie of the Federal Republic of Germany, the Swiss National Science Foundation, and the US National Science Foundation.

REFERENCES

[1] A. Kreissl, Thesis, University of Karlsruhe, Kernforschungszentrum Karlsruhe KfK 4128 (1986).

[2] A. Kreissl et al., Antiproton 1986: Proc. 8th European Symposium on Nucleon-Antinucleon Interactions, Thessaloniki, 1986, eds. S. Charalambous, C. Papastefanou, P. Pavlopoulos (World Scientific, Singapore, 1987), p. 231.

[3] K.W. Ford, V.W. Hughes and J.G. Wills, Phys. Rev. **129,** 194 (1963).

[4] J.O. Eeg, M. Martinis and H. Pilkuhn, Phys. Lett. **B92,** 117 (1980).
R. Decker and M. Martinis, Hadronic Lamb shift in antiprotonic atoms, Univ. Karlsruhe Preprint TKP 87-07 (1987).

[5] H. Bethe and E. Salpeter, Quantum mechanics of one- and two-electron systems, *in* Handbuch der Physik (Springer, Berlin-Heidelberg-New York, 1957), vol. 35, p. 88.

[6] E. Borie, Phys. Rev. **A28,** 555 (1983).

[7] E. Borie, Proc. 2nd LEAR Workshop on Physics with Low-Energy Cooled Antiprotons, Erice, 1982, eds. U. Gastaldi and R. Klapisch (Plenum, New York, 1984), p. 561.

[8] H. Pilkuhn, Z. Phys. **A276,** 365 (1976).

[9] H. Pilkuhn and H.G. Schlaile, Phys. Rev. **A27,** 657 (1983).

[10] G. Bohnert et al., Z. Phys. **D2,** 23 (1986).

[11] G. Bohnert et al., Phys. Lett. **B174,** 15 (1986).

[12] D. Rohmann et al., Z. Phys. **A325,** 261 (1986).

[13] H. Poth et al., Nucl. Phys. **A466,** 667 (1987).

[14] U. Raich, Thesis, University of Karlruhe, Kernsforschungszentrum Karlsruhe KfK 3712 (1984).

[15] B. Jödicke, Diploma Thesis, University of Karlsruhe, Kernforschungszentrum Karlsruhe KfK 3933 (1985).
G. Büche, private communication.

[16] E. Borie and B. Jödicke, Kernforschungszentrum Karlsruhe, Internal Report KfK 14.02.01P11C (1985).

[17] B.L. Roberts, Phys. Rev. **D17,** 358 (1978).
B.L. Roberts et al., Nucl. Phys. **A254,** 403 (1975).

[18] E. Hu et al., Nucl. Phys. **A254,** 403 (1975).

[19] E.R. Cohen and B.N. Taylor, J. Phys. Chem. Ref. Data **2,** 663 (1973).

[20] T. Yamazaki et al., Phys. Lett. **B53,** 117 (1974).

[21] R. Abela et al., KfK Annual Report 1980/81, Kernforschungszentrum Karlsruhe KfK 3280, 3 (1982).

Table 1

Detector specifications

Detector	Area (mm^2)	Thickness (mm)	Energy range (keV)	Resolution at $\bar{p}^{208}Pb$ 11 → 10 (eV)
D1	200	7	10–430	956
D2	200	10	10–430	867
D3	200	10	10–430	794
D4	500	13	10–675	996
D5	1134	12.5	10–610	1075

Table 2

Results for the $\bar{p}$ 11 → 10 transition in ^{208}Pb (all energies in eV)

Detector	ΔE_{exp}	Stat. (syst.) error	Total error
D1	1195	13(4)	14
D2	1199	8(4)	9
D3	1177	19(4)	19
D4	1206	9(4)	10
D5	1200	9(4)	10
Total result	1199		5
Int. ratio $I_a^{circ}:I_c^{circ}$:	1.1059 ± 0.012	theor.: 1.1058	
Int. ratio $I^{1PT}:I^{circ}$:	3.8 ± 1.1%		

Figure captions

Fig. 1 : Level and transition scheme in $\bar{p}^{208}Pb$

Fig. 2 : The $\bar{p}$ 11 → 10 transition in ^{208}Pb (detector D2)

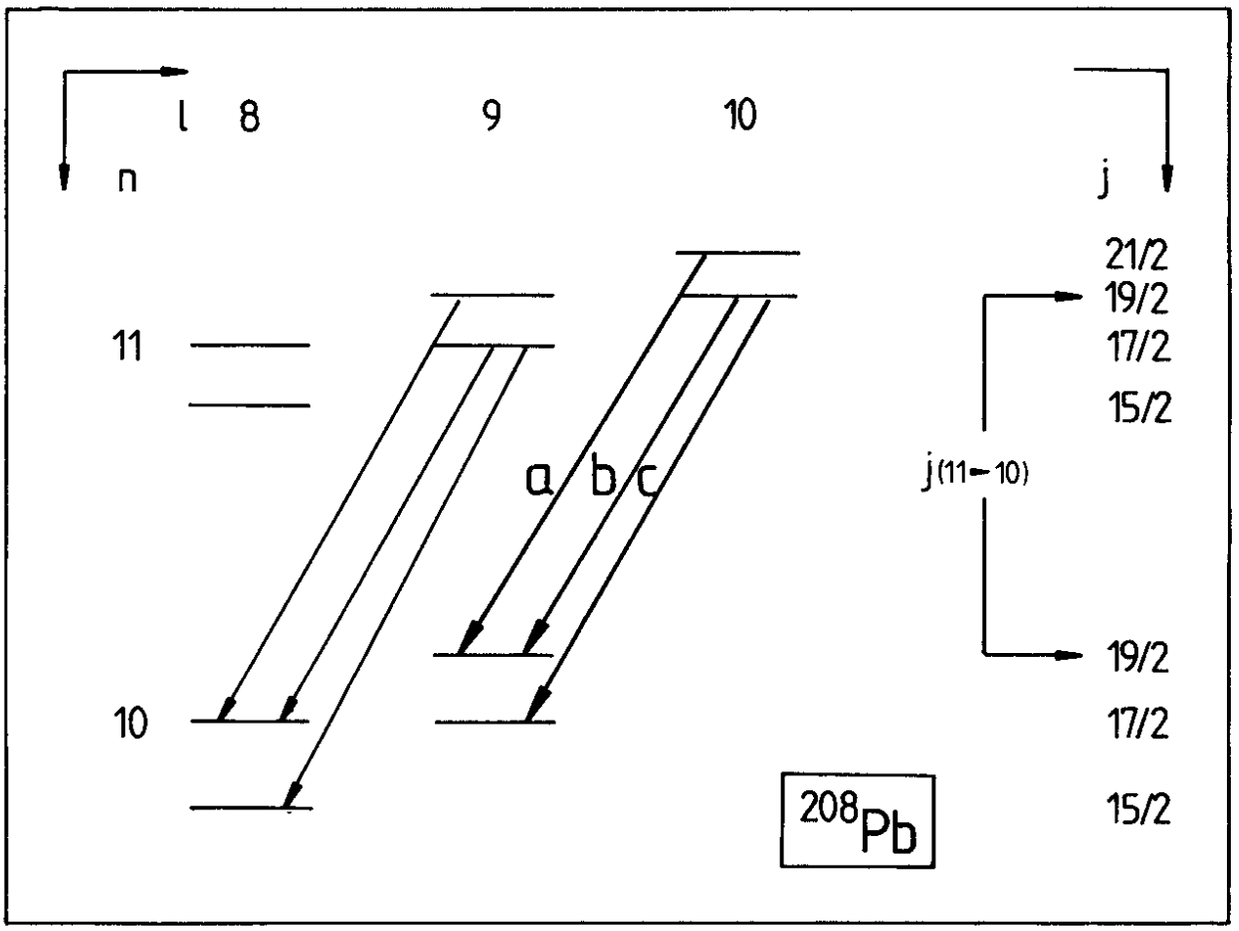

Fig. 1

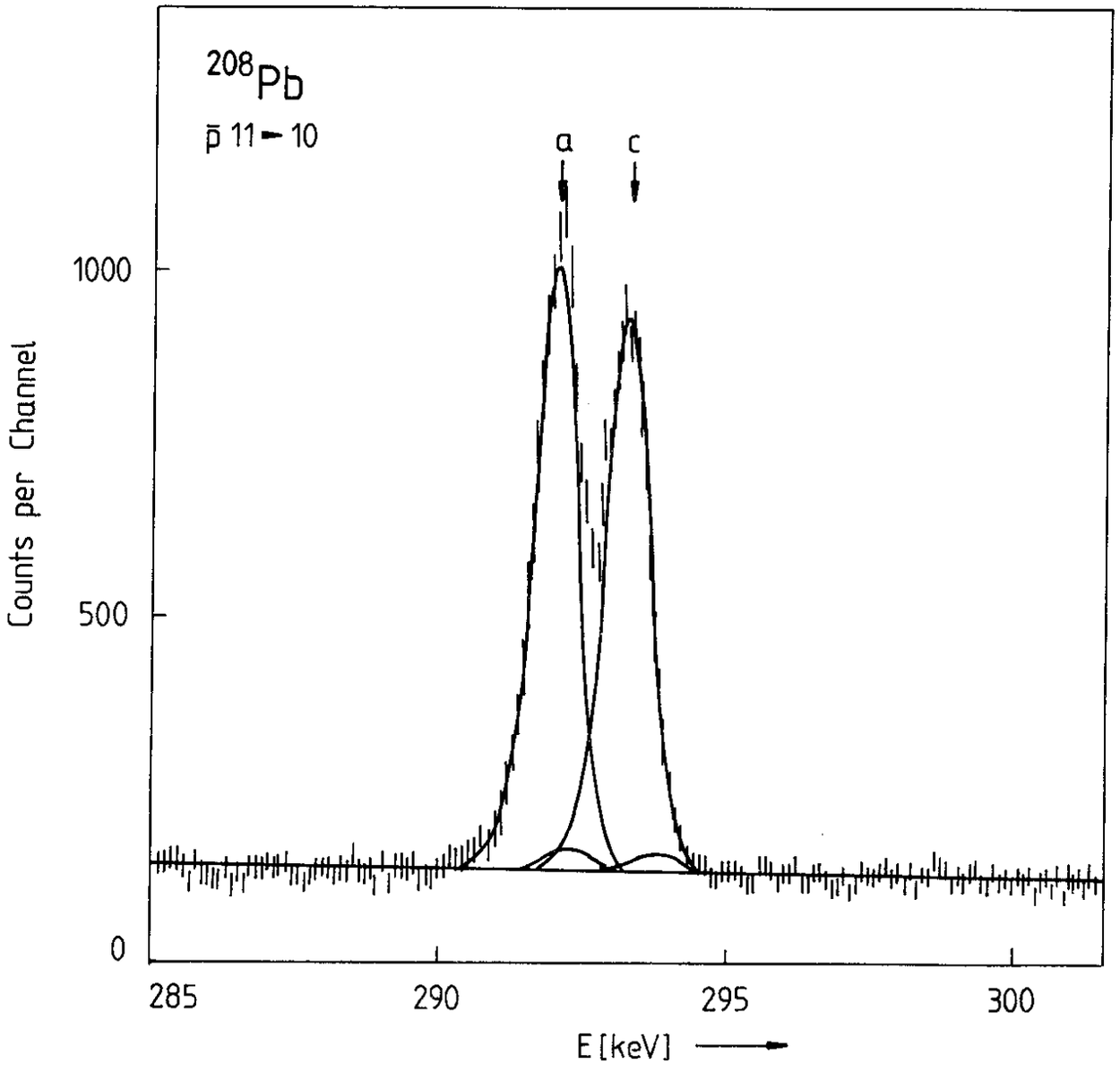
208Pb
p̄ 11 → 10
a
c
1000
500
0
Counts per Channel
285
290
295
300
E [keV]

Fig. 2